CORRELATIONS BETWEEN MOLECULAR (RAMAN) AND MACROSCOPIC (RHEOLOGY) DATA FOR PROCESS MONITORING OF THERMOSET COMPOSITES

Stuart Farquharson and Wayne Smith
Real-Time Analyzers
East Hartford, CT

Jennifer Rose
Bohlin Instruments, Inc.

Montgomery Shaw
Polymer Program and Department of Chemical Engineering
Institute of Materials Science
University of Connecticut
Storrs, CT

ABSTRACT

The superior strength-to-weight ratio of fiber-reinforced polymer matrix composites make them suitable for applications ranging from sporting goods to aircraft components. However, consistent fabrication of components with desired mechanical properties has proven difficult and has led to high production costs. This is largely due to the inability to monitor and control polymer cure, which chemically is the process of polymer chain extension and cross-linking. Optimized process control with minimum waste will require a sensor to gather real-time process data, a cure model based on reaction mechanisms and physical changes, correlations between molecular structure and macroscopic properties, and an expert system to control the fabrication device. This paper presents simultaneous rheology and Raman measurements during the cure of diglycidyl ether of bisphenol A by triethyl tetramine (an epoxy resin). Correlations between molecular reaction kinetics and physical property changes are developed, forming the basis of a cure model.

INTRODUCTION

The superior engineering properties of fiber-reinforced polymer matrix composites, primarily the high strength-to-weight ratio, make them suitable for applications ranging from sporting goods to aircraft components (*e.g.* helicopter blades)[1-3]. Thermoset composites are primarily manufactured in two steps: preparing a pre-impregnated (prepreg) and molding the part. Prepregs are prepared from a woven sheet of reinforcement fiber (carbon, glass, or aramid) prepreg with one or more matrix components (usually a partially cured thermoset polymer or thermoplastic). The chemical structure of a prepreg thermoset resin based on diglycidyl ether of bisphenol A (DGEBA) is shown in Figure 1. DGEBA based composites are widely used because thermosets containing substituted aromatic rings have high resistance to thermal degradation and chemical attack[1,2].

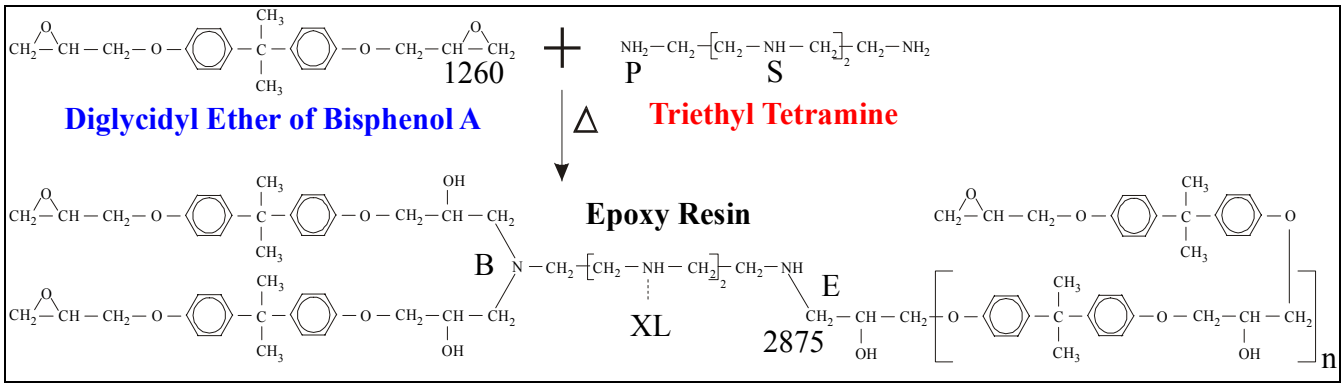

Figure 1. Chemical structures and cure reaction of DGEBA by TETA. Possible reaction mechanisms include the epoxy oxirane ring with 1) the primary amine (P) resulting in chain extension (E); 2) the newly formed secondary amine resulting in branching (B) or; 3) the mid-molecule secondary amines resulting in cross-linking (XL).

The prepreg is then shaped and cured in a combination heat and molding device. For an autoclave, prepreg sheets are cut and layered on a metal form plate (caul), enclosed in a vacuum bag, and cured according to the manufacturer's schedule[4]. This schedule is based on pre-determined, off-line measurements such as dynamic mechanical rheology[5]. The isothermal cure of a thermoset resin can be characterized in terms of gelation and vitrification. Gelation is generally defined as the transformation of the resin from the liquid to rubbery state, while vitrification is the transformation from the rubbery state to the glass state. Gelation and vitrification experiments are often used to develop a time-temperature-transformation (TTT) diagram. Essentially, a series of rheology measurements are performed at various isothermal cure temperatures. The gel and vitrification times can be calculated from the measured storage (G') and loss moduli (G"), as a maximum in G" and a maximum in G"/G', respectively[6,7]. Vitrification follows an S-shaped curve in the TTT diagram due to the chemical kinetics (which increase with temperature) and the physical changes that slow the reaction (*e.g.* increasing molecular weight). For a given isothermal cure, the vitrification point represents the cessation of reaction, as the increased viscosity and/or molecular weight prevent further reactive group interactions. A generalized diagram developed for the cure of DGEBA with amine is shown in Figure 2[8].

Ideally, the TTT diagram aids a manufacturer in selecting a heat schedule to produce a cured resin with the desired properties. The key temperature is the gel Tg (Tg_{gel}); a resin cured below this temperature will predominantly contain long-chains and will be more ductile, whereas above this temperature the converse is true (higher cross-linking, more brittle). Below the Tg_{gel}, a resin system can be cured such that it will vitrify, but not gel. This is the desired effect in preparing prepregs. The resin system is hardened (vitrified), but not completely cured (gelled or cross-linked). In this state (B-stage) the reaction is not complete. An increase in temperature can soften the resin (lower viscosity) such that a partially cured resin can be further processed and cured. The S-shaped vitrification curve can be used to select a cure temperature to prepare a prepreg with the desired extent-of-cure and toughness[9,10]. Nevertheless, even with a well developed TTT diagram, consistent fabrication of components within specifications has proven difficult and led to high production costs[11,12]. This is often attributed to slight variations in the pre-polymer formulations that influence reaction mechanisms. For example, a prepreg that has matured during storage may have a higher than usual content of pre-extended base resin. This would decrease the amount of cross-linking for a pre-selected cure temperature resulting in a product that is more pliable than desired. Also, the TTT diagram is only valid for isothermal cures, and manufacturing practices usually include temperature ramps.

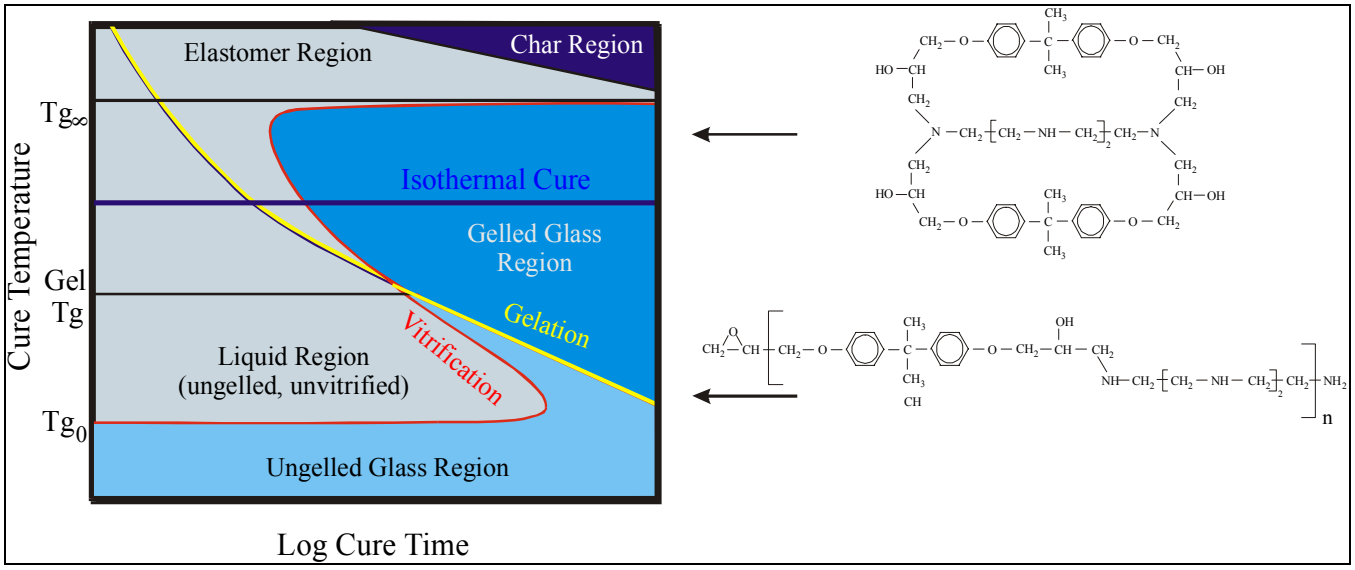

Figure 2. Generalized Time Temperature Transformation diagram based on isothermal cure of DGEBA with TETA. Note regions and gelation and vitrification curves. Chemical structures are included to indicate the extreme cases of predominantly cross-linked (top) and chain extension (bottom). Diagram redrawn from reference 8.

In recent years, researchers have been investigating fiber optic based spectroscopies to monitor polymer and composite cure in real-time. This includes fluorescence[13,14], near infrared[15], infrared[16], and Raman spectroscopies[17,18]. Raman measurements have been very successful at monitoring the cure of epoxy resins and at least one measurement of composite cure has been performed in an industrial autoclave[19]. However, only limited studies employing infrared[8], nuclear magnetic resonance[20], and Raman spectroscopy[21,22] have been performed to develop the necessary correlations between molecular kinetics and physical properties required to achieve process control. In an effort to develop the required correlations, fiber optics have been integrated into a parallel plate rheometer to collect Raman spectra simultaneous to rheology data. These simultaneous measurements during the cure of diglycidyl ether of bisphenol A by triethyl tetramine are presented in this paper.

EXPERIMENTAL

DGEBA and TETA were obtained from the Dow Chemical Company (Midland, MI) and used without modification. The samples, consisting of a 14 to 100 weight percent TETA to DGEBA, were mixed at room temperature and placed between two 25 mm diameter aluminum parallel plates set 2.0 mm apart, just prior to measurements. The storage and loss moduli of the polymer samples were measured using the dynamic head of a Rheometrics System IV (Rheometrics, Piscataway, NJ). The rheometer was used to isothermally heat the samples, while a servo motor supplied an oscillating (ω, sinusoidal) torsional strain (γ) to the upper plate and the response was measured by a transducer in the lower plate as torque (τ) or stress. The strain was automatically adjusted between 0.3 and 50% to maintain the torque within the optimum signal range (1-10 rad/s). These parameters and the response lag time (or phase angle, δ) were used to calculate the elastic (storage) modulus and the viscous (loss) modulus defined as $G' = (\tau_o/\gamma_o)\cos\delta$ and $G'' = (\tau_o/\gamma_o)\sin\delta$, respectively. These values were then used to calculate the gel time ($dG''/dt = 0$) and vitrification time ($d\tan\delta/dt = 0$) as well as the complex viscosity magnitude defined as $|\eta^*| = [(G'^2 + G''^2)]^{1/2}/\omega$. This viscosity is particularly useful because it correlates well with steady-flow viscosity, at least at low degrees of cure. These measurements and calculations were performed for a series of samples cured isothermally at 25-70°C in 5°C increments (measured temperatures varied by 1° or 2°C).

The fiber optic probe consisted of a simple side-by-side arrangement, employing 3 m of a 200 µm-diameter source fiber and a 365 µm diameter collection fiber (low OH^-, hard clad Spectran Specialty Optics, Avon, CT). The fibers were inserted through a drilled hole in the upper parallel plate at a 25° angle from normal to minimize back reflections (Figure 3). The fibers were fixed with epoxy resin (ND 353, Epotek, Billerica, MA) and polished smooth with 0.5 µm alumina paper between each isothermal cure measurement (Buehler, Lake Bluff, IL). To ensure that the probe was not damaged and measurements were consistent from one experiment to another, the throughput of the source fiber and the collection efficiency of the return fiber were measured prior to each cure measurement. It was found that nearly 65% of the 1-W laser source entry power reached the sample, while the spectral intensity of a glass vial of toluene placed against the fibers at the face of the parallel plate varied by less than 10% from measurement to measurement.

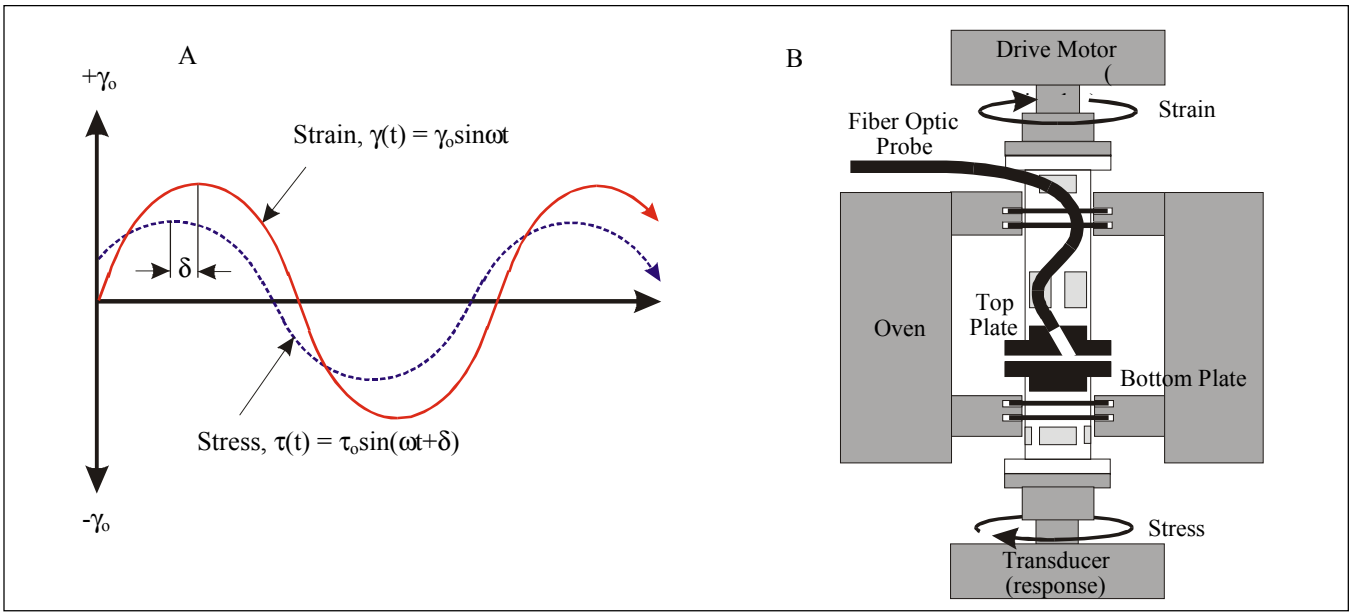

Figure 3. A) The phase relationship between the applied stress and the measured strain and; B) Schematic of a parallel-plate rheometer (including fiber optic probe interface).

A prototype Fourier transform Raman spectrometer (Real-Time Analyzers, RTA, East Hartford, CT) was used for these measurements[23]. The system consisted of a Nd:YVO_4 laser (Spectra Physics, Palo Alto, CA) for excitation at 1064 nm, an interferometer built by Online Technologies (OLT, East Hartford, CT) for frequency separation, an uncooled InGaAs detector for signal detection (RTA), and an Intel 400-MHz Pentium II based laptop computer (Dell, Round Rock, TX) for interferometric control, data acquisition (OLT), and analysis (LabVIEW by National Instruments, Austin, TX). Additional components included a notch filter (Kaiser, Ann Arbor, MI) and interferometer entrance and exit optics (Edmund Scientific, Barrington, NJ). This design allowed spectral acquisition from -950 (anti-Stokes) to 3500 cm^{-1} (Stokes) per scan. The FT-Raman spectrometer has been specifically designed for industrial applications; it is immune to factory floor vibrations, shock, and temperature drift and also performs continuous self-diagnostics. This eliminates long term spectral intensity drift while the HeNe wavelength reference laser provides high wavelength accuracy (Connes advantage)[24], allowing reliable analysis of spectra (*e.g.* peak height).

A LabVIEW program was written that displayed each spectrum as it was collected and a false intensity color scale of sequential spectra that was continually updated (Figure 4). The program also allowed the selection of a spectral feature (peak height, integrated area, or region), correcting for baseline offsets (linear), normalizing it to another feature, and plotting it as a function of cure time. Once several data points were collected, they could be fit to a model to determine a projected or final rate constant. The acquired spectra could also be continually displayed (movie mode) to monitor trends in real-time. All these operations and the collection of data could be performed simultaneously.

RESULTS AND DISCUSSION

The measurement of the storage modulus, G', the loss modulus, G", and the calculated vitrification, tan δ, and complex viscosity, $|\eta^*|$ are shown in Figure 5 for the isothermal cure of the epoxy resin at 26°C. As expected, the moduli and viscosity increase as the resin cures and the molecular weight increases. The loss modulus passes through a maximum at 222 minutes defining the gelation time. Similarly, the ratio of the loss to the storage moduli passes through a maximum at 105 minutes defining the vitrification time.

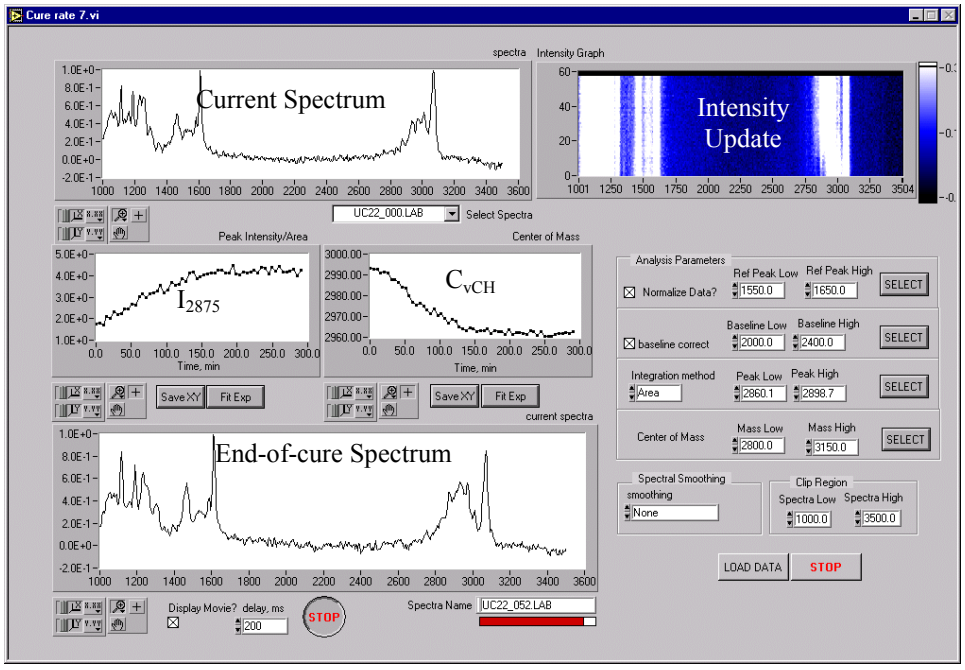

Figure 4. Display of Cure Rate program. Top row shows active spectral acquisition (first cure spectrum displayed), and false intensity color scale of spectra already collected (note shift of CH bands near 3000 cm^{-1}). Middle row shows peak/area intensity and center-of-wavenumber (C_v CH spectral region) as a function of cure time. Bottom row shows continuous display of collected spectra (movie, end-of-cure spectrum displayed). All parameters and features can be selected and displayed simultaneous to the collection of data.

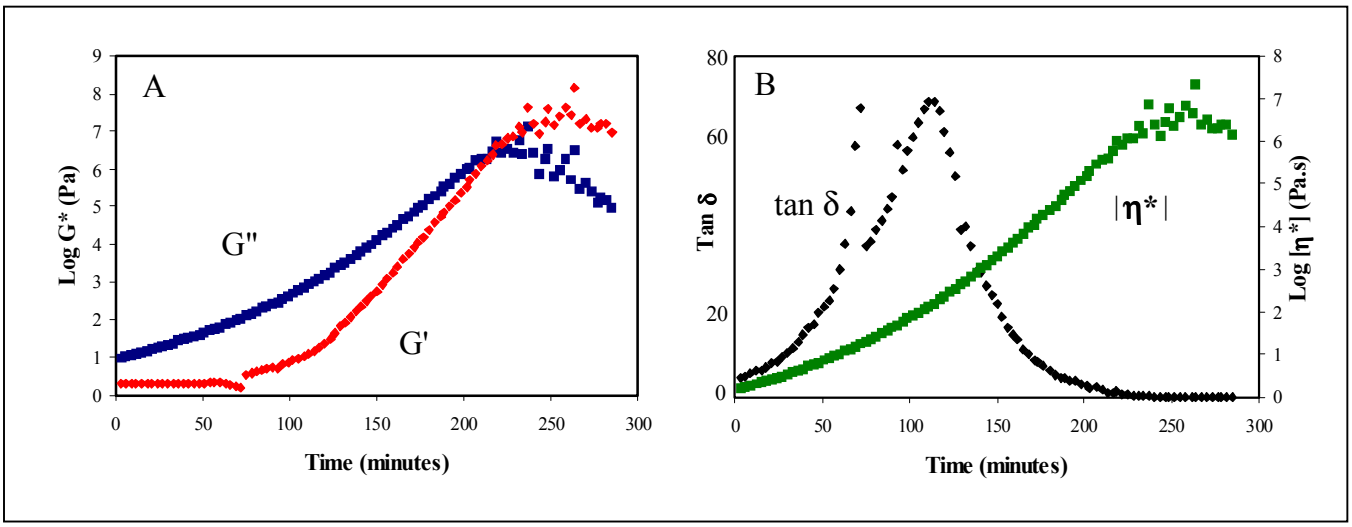

Figure 5. Viscoelastic data for isothermal cure of DGEBA and TETA 26°C. Parallel plates were 25 mm diameter, respectively. Frequency = 1 rad/s, plate gap = 2.0 mm, and strain varied from 0.001-0.1. A) Measured storage modulus, G′ (◆) and loss modulus G″ (■) during cure. B) Calculated tan δ (◆) and complex viscosity |η*| (■).

There are a number of Raman spectral bands that can be used to monitor the cure of DGEBA with TETA (Figure 6). The disappearance of both the epoxide ring stretching mode at 1260 cm^{-1}, and the antisymmetric stretch of the terminal epoxide $=CH_2$ group at 3070 cm^{-1} have been successfully used[17,22]. However, both bands overlap other bands, namely the -C-O-C- ether stretch at 1232 cm^{-1} [18,22]and the aromatic C-H stretch at 3065 cm^{-1}. Although neither band takes part in the reaction, only the latter seems unaffected by the reaction. In addition to these bands, the symmetric terminal epoxide $=CH_2$ stretch (3010 cm^{-1}) also disappears as the cure reaction proceeds, while two symmetric CH_2 stretching bands (2835 and 2875 cm^{-1}), associated with the newly formed link between the amine and epoxy, increase in intensity as the reaction proceeds. However, even when the spectra are scaled to the intensity of the 1605 cm^{-1} phenyl trigonal ring stretching mode, used here as an internal intensity reference, there is considerable scatter in the data (Figure 7A). Previously, we reported a pseudo chemometrics approach in which the general shift the C-H stretching region (2800 to 3200 cm^{-1}) to lower wavenumbers was plotted as a function of time, viz[22]:

$$C_v = \sum_{2800}^{3200}(\nu_i I_i)/\Sigma I_i, \qquad 1$$

where C_v is the center-of-wavenumber for the CH bands, and I is the intensity of the ith wavenumber ν_i (Figure 7B). The success of this approach is clearly due to the fact that C_v includes the contributions of the 2835, 2875, 3010, and 3070 cm^{-1} spectral bands, and the summation has the effect of canceling random error in the data. A similar reduction in data scattering was obtained by combining the CH_2 bands obtained by integrating the area between 2825-2895 cm^{-1} (Figure 7B).

The spectral data, either band intensities or C_v, were normalized by setting the maximum and minimum values to 1 and 0 (representing approximate initial and final values) and used to determine the extent-of-cure (α_t). Initially, the normalized data was fit with a first order decay (or growth) curve, viz:

$$\alpha_t = 1\text{-}e^{-kt} \qquad 2$$

where t is time and k is the cure rate constant. In Figure 7B, the C_v data collected for cure at 26°C fit with this equation yields a rate constant of $1.15x10^{-2}$ (normalized data, ND)/minute. However, inspection of the fit suggests that it is less than adequate in representing the measurements. The Sigmoidal shaped data is better fit with an Avrami-type equation[25], viz:

$$\alpha_t = 1\text{-}e^{-kt^2} \qquad 3$$

where time is squared. The higher power in the exponential has been reported for autocatalytic reactions[26]. In the present reaction the hydroxyl group formed by reaction of the primary amine can catalyze the reaction of the newly formed secondary amine. Recent studies support the formation of a termolecular intermediate consisting of the amine, the epoxy, and the hydroxyl groups[27]. In the present study, the newly formed hydroxyl group is located three bonds distant from the newly formed secondary amine. Rotation about these single bonds ideally locates the hydroxyl group to assist in opening the epoxy oxirane ring through hydrogen bonding and facilitate attack by the nucleophilic amine through the lone electron pair (Figure 8). This reaction mechanism suggests that the newly formed secondary amines may have a lower activation energy than the primary amines. Others have suggested that the mid-chain secondary amine activation en-

ergy is not significantly higher[8]. As can be seen in Figure 7B, fitting the data with the Avrami-type equation provides much better results (mean squared error decreased from 0.0032 to 0.0013). Furthermore, the same rate constant, 1.35×10^{-4} ND/minute, is obtained for fitting C_v, the CH_2 area (-1.35×10^{-4} ND/min), as well as the 1260, 2835, 2875, 3010, and 3070 cm^{-1} bands. Raman spectra collected at higher temperatures were also fit with Avrami-type equations with time squared. It was found that the spectral data collected at 67°C was better fit with time raised to the 2.6 power. This difference may be due to the influence of an additional reaction mechanism, possibly a bimolecular reaction of the hydroxyl group with oxirane rings, beginning to occur at this higher temperature.

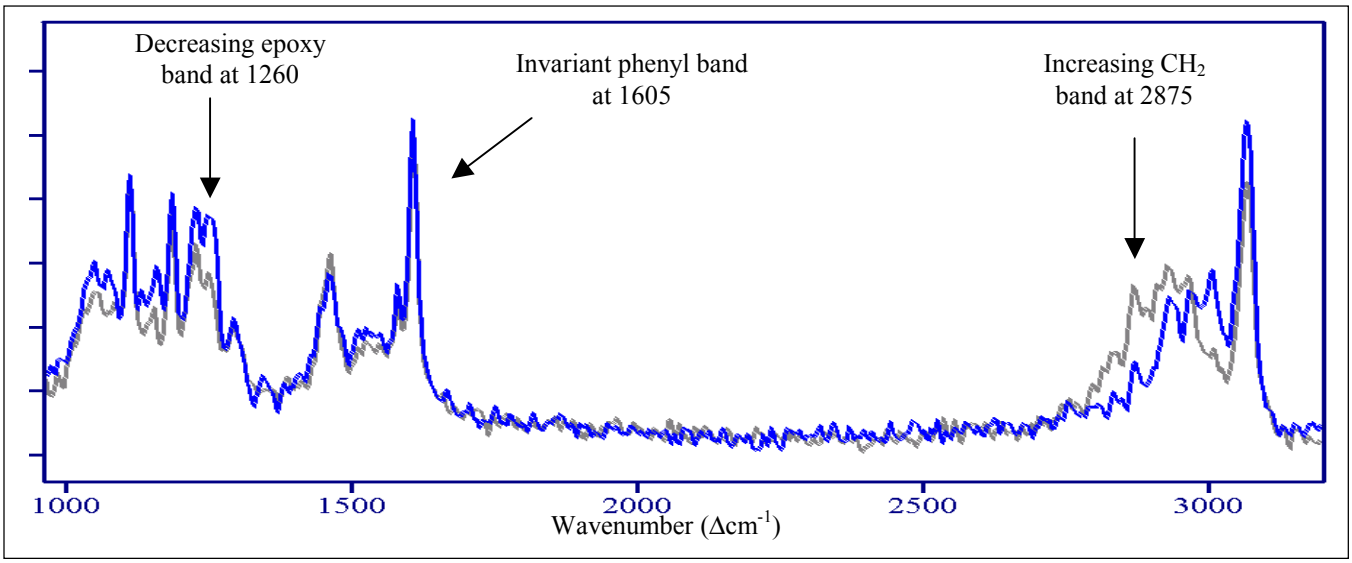

Figure 6. Raman spectra for isothermal cure of DGEBA and TETA 26°C at A) 2.5, and; B) 250 minutes into the reaction. Conditions: 500 mW of 1064 nm, side-by-side fiber optic probe, 300 averaged scans (five minutes) at 8 cm^{-1}.

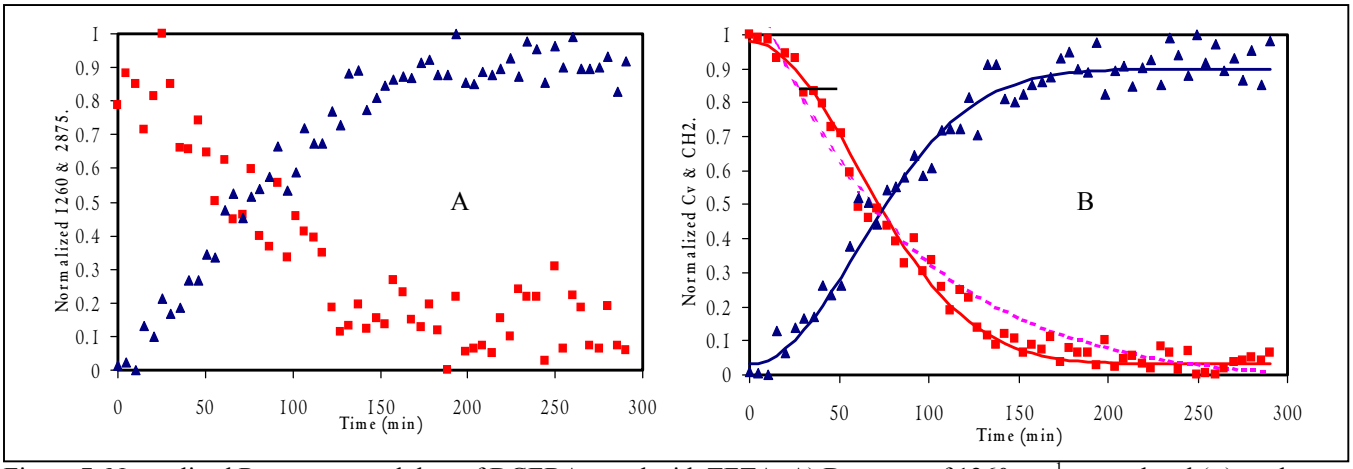

Figure 7. Normalized Raman spectral data of DGEBA cured with TETA. A) Decrease of 1260 cm^{-1} epoxy band (■), and growth of 2875 CH_2 band (Δ) intensities; B) decrease of CH center-of-mass, C_v (■) and growth of combined CH_2 bands (Δ). Curve fits generated according to Equation 2 (----) and 3 (—) described previously.

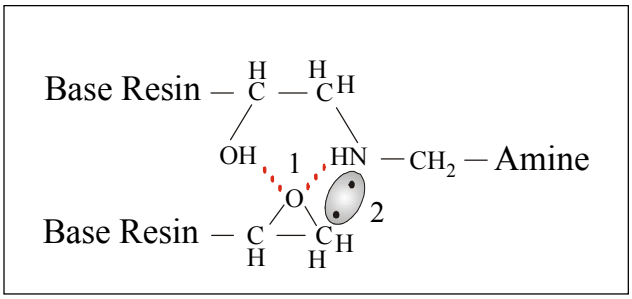

Figure 8. Illustration of termolecular intermediate. Note 1) hydrogen bonding and; 2) lone electron pair.

In an effort to draw correlations between the rheology and Raman data sets, activation energies (Ea) were calculated based on the gel times and the rate constants, according to the Arrhenius equation:

$$k = Ae^{-Ea/RT} \qquad 4$$

where A is a constant, R is the ideal gas constant (8.1344 J/K•mole), and T is absolute temperature. Plots of ln tgel (gel time) versus 1000/T and ln k versus 1000/T from 25-70°C are shown in Figure 9A. The slopes of 6.68 and 9.36 (Ea/R) correspond to activation energies of 54.3 kJ/mole (13.0 kcal/mole) and 76.1 kJ/mole (18.2 kcal/mole), respectively. Both activation energies are supported by literature values for epoxy systems. A value of 53.7 kJ/mole based on gel times has been reported[28], while a value of 69 ±6 kJ/mole based on near infrared kinetic data has been reported[26,29]. In one paper, activation energies were determined from both rheology and infrared spectroscopy for the same epoxy system (DGEBA cured with bis (*p*-amino cyclohexyl) methane). The separate measurements yielded values of 45 and 52 kJ/mole respectively. In all three literature cases, the activation energies from rheology were lower than those from spectroscopy. This difference may simply imply that the two measurements do not reflect the same phenomena. The gel time represents a change in physical state (domain formation), while the spectroscopy represents a chemical reaction (oxirane ring-amine-hydroxyl groups). Clearly the two phenomena occur at different time during cure. This suggested examining the vitrification times, which corresponds to the time when the reactions cease, and comparing it to the time when 90% of the reaction reaches completion according to the Raman kinetic data. The latter was determined by solving for **t** in the Avrami equations, *i.e.*,

$$\mathbf{t}\ (\text{min}) = [(\ln(1/0.99)/\mathbf{k}]^{1/2} \qquad 5$$

This yielded times of 130, 78, 37, and 19 minutes for cure at measured temperatures of 26°, 36°, 52°, and 67°C. Employing the Arrhenius equation, this yields an activation energy of 39.1 kJ/mole. This value is nearly identical to the activation energy of 38.6 kJ/mole determine from the vitrification times (max G"/G'). This is reasonable since the vitrification times indicate cessation of the reactions due to formation of the glass state, which might correspond to reaching 90% completion. These data, along with the gelation times and reaction rate constants determined from the Raman spectra, are summarized in Table I.

Finally, the gelation, vitrification, and 90% cure times were plotted in terms of a TTT diagram (Figure 10). The data clearly indicates that virtually all cures were performed below the Tg_{gel}, which was determined as 65°C (gel time equals vitrification time). The diagram also shows the 90% cure times to closely trend the vitrification times.

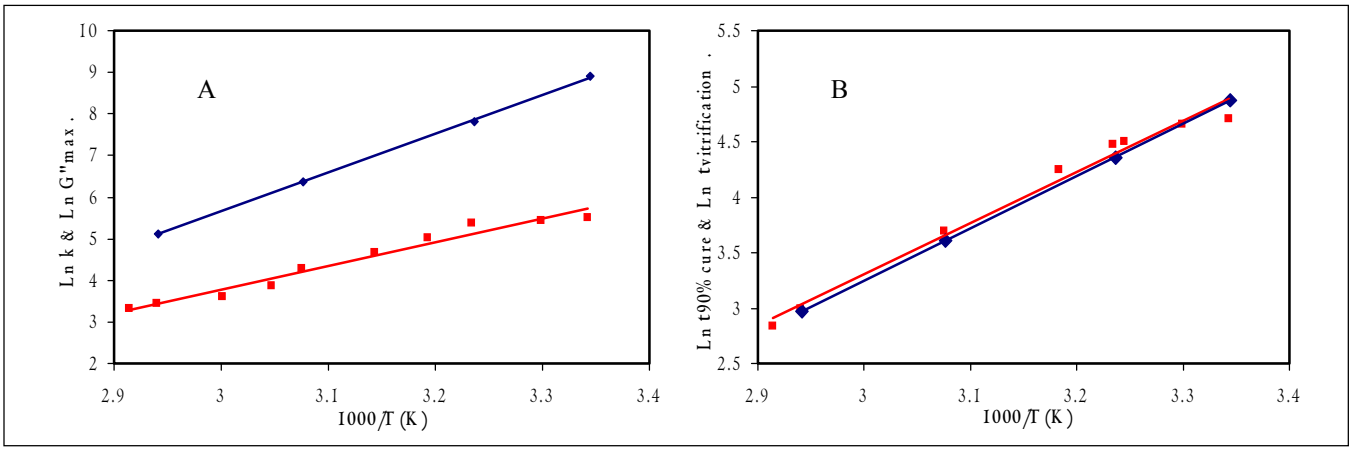

Figure 9. Activation energy obtained from the slope of a plot of the natural log of A) gel times (G"max, ■, rheology) and rate constants (k, ◆, Raman) and; B) vitrification times (G"/G' max, ■, rheology) and 90% cure (α= 0.1, Avrami rate equations, ◆, Raman) as a function of reciprocal temperature according to the Arrhenius equation.

Table I Summary of rheology and Raman data as indicated.

Temperature (°C)	Gel Time (minutes)	Vitrification Time (minutes)	90% Cure Time (minutes)	Rate Constants (minutes^{-1})
26	222	110	130	1.35×10^{-4}
30	230	105		
36	216	88	78	3.8×10^{-4}
40	150	70		
45	106			
52	68	40	37	1.7×10^{-3}
55	48			
60	37			
67	30	17	19	6.0×10^{-3}
70	25			

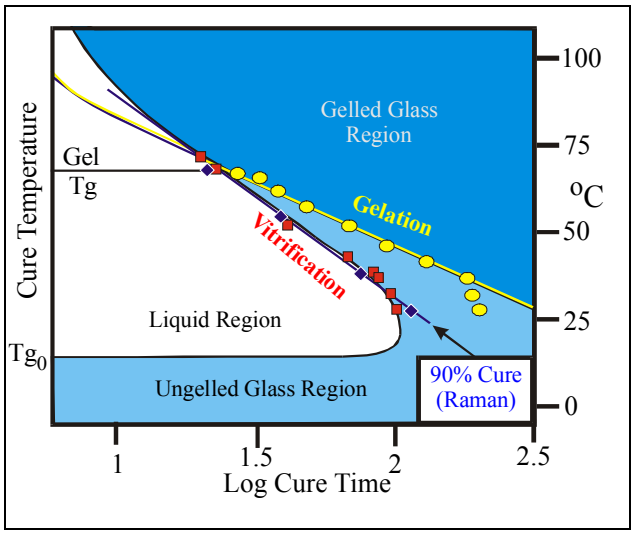

Figure 10. Time Temperature Transformation diagram based on isothermal cure of DGEBA by TETA measured here. 90% cure times (◆) based on Raman kinetic data are shown to closely match vitrification times (■) measured by rheology. Calculated gelation (●) times are included.

CONCLUSION

Simultaneous rheology and Raman spectroscopy measurements were performed during isothermal cure of an epoxy resin. An Avrami-type equation was found to more closely represent the Raman kinetic data than a simple first-order-decay equation. The rate constants obtained from these equations were used to calculate an activation energy, which was compared to an activation energy calculated from gelation times. The significantly different values forced us to conclude that the two techniques measured different phenomena. Nevertheless, consideration of the vitrification time as a measure of the cessation of reaction led us to compare it to times corresponding to 90% cure according to the Raman kinetic data. Not only are the calculated activation energies nearly identical, the times closely match as well. This data suggests a way to link macroscopic and molecular properties. This is demonstrated by incorporating the 90% cure data with the vitrification data into a TTT diagram. Such a diagram might form the basis of a molecular model to select a cure schedule (time-temperature). Finally, the ability to use the same method (Raman spectroscopy) to monitor molecular changes in real-time suggests real-time process control during manufacture of thermoset based composites.

ACKNOWLEDGEMENTS

The authors are also grateful to Dr. Richard Shuford for his continued support and interest in this work. This work was supported by U.S. Army Contract Number DAAL01-96-C-0084.

REFERENCES

1. B.Z. Jang, *Advanced Polymer Composites: Principles and Applications of Fibers*, (ASM International) 1994.
2. H. Lee and K. Neville, *Handbook of Epoxy Resins*, (McGraw Hill Book Company, New York) 1982.
3. R.A. Dickie, S.S. Labana, and R. S. Bauer, *Cross-linked Polymers: Chemistry, Properties, and Applications*, Ed., ACS Symposium Series 367 (1988).
4. See product literature from Dow Chemical (Midland, MI), Fiberite (Tempe, AZ), or Hexcel (Pleasonton, CA).
5. W.W. Bidstrup and S.D. Senturia, *Polym. Eng. Sci.*, 29, 290-294 (1989).
6. S.B. Ross-Murphy, *J. Texture Studies*, 26, 391-400 (1995).
7. C.M Tung and P.I.J. Dynes, *J. Applied Polymer Science*, 27, 4569-574 (1982).
8. J.B. Enns and J.K. Gillham, *J. Applied Polymer Science*, 28, 2567-2591 (1983).
9. H.R. Allcock and F.W. Lampe, *Contemporary Polymer Chemistry*, Chapter 21, (Prentice Hall, Englewood Cliffs NJ) 1981.
10. R.A. Sinclair, *Ultrastructure Processing of Ceramics, Glasses, and Composites*, L.L. Hench and D.R. Ulrich, Eds., 256-264, (John Wiley & Sons, New York) 1984.
11. B. Benjamin, *High-Performance Composites*, 21-22 (1993).
12. D. Wilson, *British Polymer Journal*, 20, 405-416 (1988).
13. A. Fuchs, H.J. Paix, and N.-H. Sung, *ANTEC*, 243-244 (1992).
14. X.-D. Sun and C.S.P. Sung, *ACS Polym. Preprints*, 35(1), ACS, 435-436 (1994).
15. S. Farquharson, P.B. Arnoudse, M.H. Wyckoff, and P.T. Keillor III, *SPIE*, 1172, 164-173 (1989).
16. M.A. Druy, L. Elandjian, L., W.A. Stevenson, R.D. Driver, G.M. Leskowitz, and L.E. Curtiss, *SPIE*, Vol. 1170, (1989).
17. S. Farquharson and S.F. Simpson, *SPIE*, 1681, 276-290 (1992).
18. K.E. Chike, M.L. Myrick, R.E. Lyon, and S.M. Angel, *Applied Spectroscopy*, 47, 10 (1993).
19. S. Farquharson, W. Smith, E. Rigas, and D. Granville, *SPIE*, 4201, paper number 18 (2000).
20. X. Zhang, M.G. Looney, D.H. Solomon, and A.K. Whittaker, *Polymer*, 38, 5835-5848 (1997).
21. J.R. Rose, R. Osbaldiston, W. Smith, S. Farquharson, and M.T. Shaw, *ANTEC*, 98, 939-944 (1998).
22. S. Farquharson, S. Bhat, R. Osbaldiston, M. Di-Taranto, W. Smith, J. Rose, Y-M. Liu, and M.T. Shaw, *SPIE*, 3535, 303-316 (1998).
23. S. Farquharson, W. Smith, R.C. Carangelo, and C. Brouillette, *SPIE*, 3859, 14-23 (1999).
24. J. Connes, *Rev. Opt. Theor. Instrum.*, 40, 54 (1961).
25. P.C. Heimenz, *Polymer Chemistry: The basic concepts*, Marcel Dekker, 219-225 (1984).
26. L. Xu, J.H. Fu, and J.R. Schlup, *JACS*, 116, 2821-26 (1994).
27. C.J. DeBakker, G.A. George, N.A. St John, and P.M. Fredericks, *Spectrochimica Acta*, 49A, 739-752 (1993).
28. M. Arellano, P. Velazquez, and V.M. Gonzalez-Romero, *SPE Antec* , 838-842 (1989).
29. M.B. Roller, *Poly. Eng. Sci.*, 26 432-440 (1986).